The docking domain of histone H2A is required for H1 binding and RSC-mediated nucleosome remodeling

Manu Shubhdarshan Shukla[1,2], Sajad Hussain Syed[1,2], Damien Goutte-Gattat[1], John Lalith Charles Richard[1,2], Fabien Montel[3], Ali Hamiche[4], Andrew Travers[5,6], Cendrine Faivre-Moskalenko[3], Jan Bednar[7,8,9], Jeffrey J. Hayes[10], Dimitar Angelov[2,*] and Stefan Dimitrov[1,*]

[1]Université Joseph Fourier - Grenoble 1; INSERM Institut Albert Bonniot, U823, Site Santé-BP 170, 38042 Grenoble Cedex 9, [2]Université de Lyon, Laboratoire de Biologie Moléculaire de la Cellule, CNRS-UMR 5239/INRA 1237/IFR128 Biosciences, Ecole Normale Supérieure de Lyon, [3]Université de Lyon, Laboratoire de Physique (CNRS UMR 5672) Ecole Normale Supérieure de Lyon, 46 Allée d'Italie, 69007 Lyon, [4]Institut de Génétique et de Biologie Moléculaire et Cellulaire, CNRS/INSERM/ULP, Parc d'innovation, 1 rue Laurent Fries, 67404 Ilkirch Cedex, France, [5]MRC Laboratory of Molecular Biology, Hills Road, Cambridge CB2 2QH, UK, [6]Fondation Pierre-Gilles de Gennes pour la Recherche, c/o LBPA, École Normale Supérieure de Cachan, 61 Avenue de Président Wilson, 94235 Cachan Cedex, France, [7]Institute of Cellular Biology and Pathology, First Faculty of Medicine, Charles University in Prague, [8]Department of Cell Biology, Institute of Physiology, Academy of Sciences of the Czech Republic, Albertov 4, 128 01 Prague 2, Czech Republic, [9]CNRS, Laboratoire de Spectrometrie Physique, UMR 5588, BP87, 140 Av. de la Physique, 38402 St. Martin d'Heres Cedex, France and [10]Department of Biochemistry and Biophysics, University of Rochester School of Medicine and Dentistry, Rochester NY 14642, USA

ABSTRACT

Histone variants within the H2A family show high divergences in their C-terminal regions. In this work, we have studied how these divergences and in particular, how a part of the H2A COOH-terminus, the docking domain, is implicated in both structural and functional properties of the nucleosome. Using biochemical methods in combination with Atomic Force Microscopy and Electron Cryo-Microscopy, we show that the H2A-docking domain is a key structural feature within the nucleosome. Deletion of this domain or replacement with the incomplete docking domain from the variant H2A.Bbd results in significant structural alterations in the nucleosome, including an increase in overall accessibility to nucleases, un-wrapping of ~10 bp of DNA from each end of the nucleosome and associated changes in the entry/exit angle of DNA ends. These structural alterations are associated with a reduced ability of the chromatin remodeler RSC to both remodel and mobilize the nucleosomes. Linker histone H1 binding is also abrogated in nucleosomes containing the incomplete docking domain of H2A.Bbd. Our data illustrate the unique role of the H2A-docking domain in coordinating the structural-functional aspects of the nucleosome properties. Moreover, our data suggest that incorporation of a 'defective' docking domain may be a primary structural role of H2A.Bbd in chromatin.

INTRODUCTION

Eukaryotic chromatin is a highly dynamic structure, which regulates the functional aspects of the genome through its different structural states. Nucleosomes constitute the fundamental building blocks of chromatin and consist of an octamer of core histones containing two

---

copies each of H2A, H2B, H3 and H4, around which 146 bp of DNA is wound in ~1.65 superhelical turns (1). A fifth histone, termed the linker histone, is associated with the linker DNA, which determines the trajectory of incoming and outgoing linker DNAs and facilitates interaction among neighboring nucleosomes (2,3). The binding of linker histones to nucleosomes is a major *in vivo* determinant of chromatin condensation (4). The core histones are comprised of a structured histone fold domain and unstructured NH_2-termini (5). The linker histones and the NH_2-termini of the core histones as well as their posttranslational modifications are required for the proper organization of both the chromatin fiber and the mitotic chromosomes (6–9). It is becoming increasingly clear now that the structural properties of individual nucleosomes dictate the local structure of chromatin, which may lead to specialized functional zones (10–12).

Two well-known modes to modulate individual nucleosome properties are covalent modifications (acetylation, methylation, ubiquitination, etc.) of core histones and ATP-dependent chromatin remodeling (13). An emerging concept in regulation of chromatin dynamics is incorporation of core histone variants within the nucleosome (14,15). Histone variants are non-allelic isoforms of conventional histones (2). The primary structure of histone variants shows various degrees of homology with the corresponding conventional major histone species. Incorporation of histone variants imparts new structural and functional properties to nucleosomes (12,16–26). The histone H2A family encompasses the greatest diversity of variants among core histones (14,27).

The members of the histone H2A family (H2A.1, H2A.X, H2A.Z, mH2A, H2A.Bbd, H2AL2) show significant sequence variability at both NH_2- and COOH-termini (28,29). While the implications of NH_2-terminal heterogeneity still remain unclear, most of the recent work has been focused on COOH-terminal domain variations (12,16,17,21,24). Initially, it was demonstrated that the carboxyl terminal tail of H2A is essential for the stability of nucleosomal particles and that the H2A–H2B dimer displays a significant decrease in the affinity for the $(H3–H4)_2$ tetramer when the terminal 15 amino acids are removed by an endogenous protease (30). Interestingly, one of the latest described H2A variants, H2A.Bbd, exhibits a similar COOH-terminal truncation, i.e. an absence of both the COOH terminus and the very last segment of the docking domain which spans amino acids 82–119 in conventional H2A) (31).

Nucleosomes-containing H2A.Bbd exhibit significant structural alterations, including a more relaxed structure and organization with only ~130 bp of DNA in tight association with the core histones, in contrast to ~147 bp in canonical nucleosome core particles (NCPs), suggesting release of ~10-bp nucleosomal DNA from each end of the octamer (19). Moreover, the H2A.Bbd–H2B dimer is less strongly associated with the H3/H4 tetramer resulting in lower stability of nucleosomes containing this variant (12,16,17,24). These reports suggest that the docking domain of H2A might be a key feature in maintaining the native structural and functional properties of the nucleosome.

In this work, we have elucidated the role of the docking domain of H2A in nucleosome remodeling and linker histone binding, two major factors which regulate chromatin dynamics. By using a series of COOH-truncated H2A mutants we show that the docking domain of H2A is required for both nucleosome remodeling and mobilization by RSC. In agreement with this, we found that RSC was unable to mobilize nucleosomes-containing H2A. ddBbd, a chimera of the histone-fold domain of H2A fused to the incomplete and significantly divergent docking domain of H2A.Bbd. We also demonstrate that the docking domain of H2A.Bbd induces strong alterations in nucleosome structure, resulting in the inability of linker histone H1 to bind to nucleosomal arrays containing this mutant and the abrogation of nucleosome remodeling by RSC.

MATERIALS AND METHODS

Preparation of DNA probes

The 255-bp DNA probe was PCR amplified from pGEM-3Z-601 plasmid containing 601 positioning sequence in the middle (kindly provided by J. Widom and B. Bartholomew).The 5′-end labeling was performed by using ^{32}P-labeled primer in the PCR. For 'One Pot Restriction enzyme Assay' a set of eight pGEM-3Z-601.2 mutants were used as a template, each containing *Hae* III site at a different superhelical location, as described before (39). Briefly, a 278-bp fragment was amplified by PCR and 5′-end labeling was performed. Labeling of the fragment was done as described above. For DNaseI and •OH footprinting a *Not*I restricted 205-bp 601 fragment was 3′-labeled using Klenow enzyme with α-^{32}P-CTP in the presence of 50 µM dGTP. All the DNA fragments were purified on 6% Native acrylamide gel prior to use for nucleosome reconstitutions. The 255-bp cold 601.1 DNA was amplified using PCR for reconstitution of nucleosomes used in AFM experiments. For H1-binding band-shift experiment, a 189-bp was PCR amplified and body labeled using α-^{32}P CTP. For hydroxyl radical footprinting and Electron Cryo-Micrsocpoy (EC-M) to examine H1 binding, respective dinucleosomal and trinucleosomal DNA substrates were preapared as described (32).

Proteins

pET3a, containing *Xenopus laevis* H2A between *NdeI* and *BamHI* sites was used as the parent clone for contsruction of H2A C-terminal deletion mutants. ORFs corresponding to H2A Δ109, Δ97, Δ90 and Δ79 were PCR amplified and cloned into *NdeI* and *BamHI* digested pET3a vector H2A.ddBbd chimera was generated as described (19). All the recombinant histone proteins including full length *X. laevis* H2A, H2B, H3 and H4 were expressed in form of inclusion bodies in *Echerichia coli* Strain BL21(DE3) and purified as described (33). Yeast RSC complexes were purified as described (34). Full length human H1.5 clone was expressed in *E. coli* BL21-RIL strain and purified by SP-sepharose, followed by a second-step purification on Resource S cation exchange column. Mouse NAP-1

(mNAP-1) was also bacterially expressed and purified by Resource Q anion exchange column.

Nucleosome reconstitutions

Nucleosome reconstitution was performed by the salt dialysis procedure (35). Briefly, 2.4 μg Chicken erythrocyte Carrier DNA (200 bp average size) and 100 ng of either ^{32}P-labeled 255-bp 601, *Not*I restricted 601.1 fragment, 189-bp 601 DNA or an equimolar mixture of eight different 278-bp 601.2 mutant DNA fragments (100 ng) were mixed with equimolar amount of histone octamer in Nucleosome Reconstitution Buffer (NRB) 2 M NaCl, 10 mM Tris (pH 7.4), 1 mM EDTA, 5 mM β MeEtOH. Reconstitutions with unlabeled 255- and 623-bp unlabeled 601 DNA were also performed in absence of carrier DNA. In case of nucleosome reconstitutions with H2A deletion mutant or H2A.ddBbd proteins, H2A was replaced by an equimolar amount of corresponding protein in the histone octamer. All the nucleosome reconstitutions were verified on 5% native PAGE run with 0.25X TBE.

DNaseI and hydroxyl radical footprinting

The 30 ng of nucleosomes, reconstituted on *Not I* digested 601 fragment, were digested with DNaseI in a volume of 7.5 μl buffer (10 mM Tris pH 7.4, 2.5 mM MgCl₂, 1 mM DTT, 100 μg/ml BSA, 50 mM NaCl, 0.01% NP40) for 2.5 min at room temperature. Additionally 1 μg of plasmid DNA was added to the reaction mixture. Increasing amounts of DNase I (0.2, 0.3 and 0.45 units, respectively) were added to reactions. Reactions were arrested by adding 100 μl of 0.1% SDS and 20 mM EDTA. Hydroxyl radical footprinting was performed as essentially as described (36). DNA was phenol: choloroform extracted, precipitated and run on 8% denaturing PAGE. Gels were dried, exposed and imaged on phosphorimager (Fuji-FLA5100). •OH footprinting on H1 deposited dinucleosomes was performed as described (32).

AFM analysis

For the AFM imaging, 255 bp centrally positioned nucleosomes containing either H2A or H2A.ddBbd were immobilized onto APTES-mica surfaces as described previously. Image acquisition and analysis was done and DNA-complexed length (L_c) and position (ΔL) distributions were constructed as described (19,37).

H1 deposition

Full length human H1.5 was mixed with mNAP-1 in a 1:2 molar ratio (20 mM Tris–HCl, pH 7.5/0.5 mM EDTA, 100 mM NaCl, 1 mM DTT/10% glycerol, 0.1 mM PMSF) and incubated at 30°C for 15 min. These H1-mNAP1 complexes were then added increasing molar ratios (0.9, 1.25, 2.0) to nucleosomes (50 ng) reconstituted on 189-bp 601 DNA and incubated for another 15 min at 30°C. Biding efficiency was checked on a 2% agarose gel (0.25X TBE). For the E-CM experiments, a molar ratio of 1:2 (Trinucleosome: H1/Nap1) was used.

EC-M

Histone H1 was deposited on to trinucleosomes as described above. The final reaction mixes (with or without H1) were concentrated to 200 ng/ml of DNA. Samples were prepared for cryo-electron microscopy essentially as described (19,32). A 3-μl droplet of the solution was deposited on an electron microscopy grid with homemade perforated supporting film with surface treated by successive evaporation of carbon and platinum/carbon layers. The grid was immediately plunged into liquid ethane (−183°C) after removing the excess of the solution by brief blotting using Whatman No 1 filter paper. The Grid was transferred into Tecnai G2 Sphera 20 electron microscope using Gatan 626 cryotransfer holder. Sample was visualized at 80 kV acceleration voltage and images were recorded on Gatan Ultrascan1000 slow scan CCD camera at microscope nominal magnification either 14500× or 25000× (final pixel size 0.7 and 0.4 nm) with 2.5 μm underfocus.

Nucleosome mobilization and remodeling assays

Nucleosome moblilization reactions were performed with 30 ng of nucleosomes in remodeling buffer (RB) 10 mM Tris pH 7.4, 5% glycerol, 1 mM rATP, 2.5 mM MgCl₂, 1 mM DTT, 100 μg/ml BSA, 50 mM NaCl, 0.01% NP40) in a volume of 7.5 μl at 29°C. RSC units were defined as described before (38). Nucleosomes were incubated with increasing amount of RSC for 45 min. Reactions were arrested by addition of 0.01 units of apyarse. Reaction products were resolved on 5% native PAGE. Gels were run in 0.25X TBE at room temperature and processed as described above. Sliding efficiency of indicated nucleosomes were calculated from quantification of gel scans. Remodeling assays were performed on nucleosomes reconstituted on *Not I* restricted 205-bp fragment (described above). Reaction conditions were similar to the nucleosome mobilization assays. Briefly, nucleosomes were remodeled in presence of 2.4 units of RSC for indicated time points and reactions were arrested by addition of addition of 0.01 units of apyrase and 1 μg plasmid DNA. Nucleosomes were then digested with 0.5 units of DNase I, processed and analysed as described above.

RESULTS

Deletion or alteration of the COOH-terminal region of H2A results in structural perturbations in the nucleosome

In order to understand the role of the COOH-terminal portion of H2A and the H2A-docking domain in nucleosome structure, we made serial COOH-deletion mutants using the *X. laevis* H2A protein as the parent clone (Figure 1A and Supplementary Figure S1A). Note that in the Δ79 H2A mutant, both the docking domain and the COOH-terminus of H2A were completely deleted (Figure 1A and B). A chimeric protein, H2A.ddBbd, in which the docking domain of H2A was replaced with the docking domain of H2A.Bbd, was also constructed (Figure 1A). As controls, full length H2A and H2A.Bbd were used. All proteins were bacterially expressed and
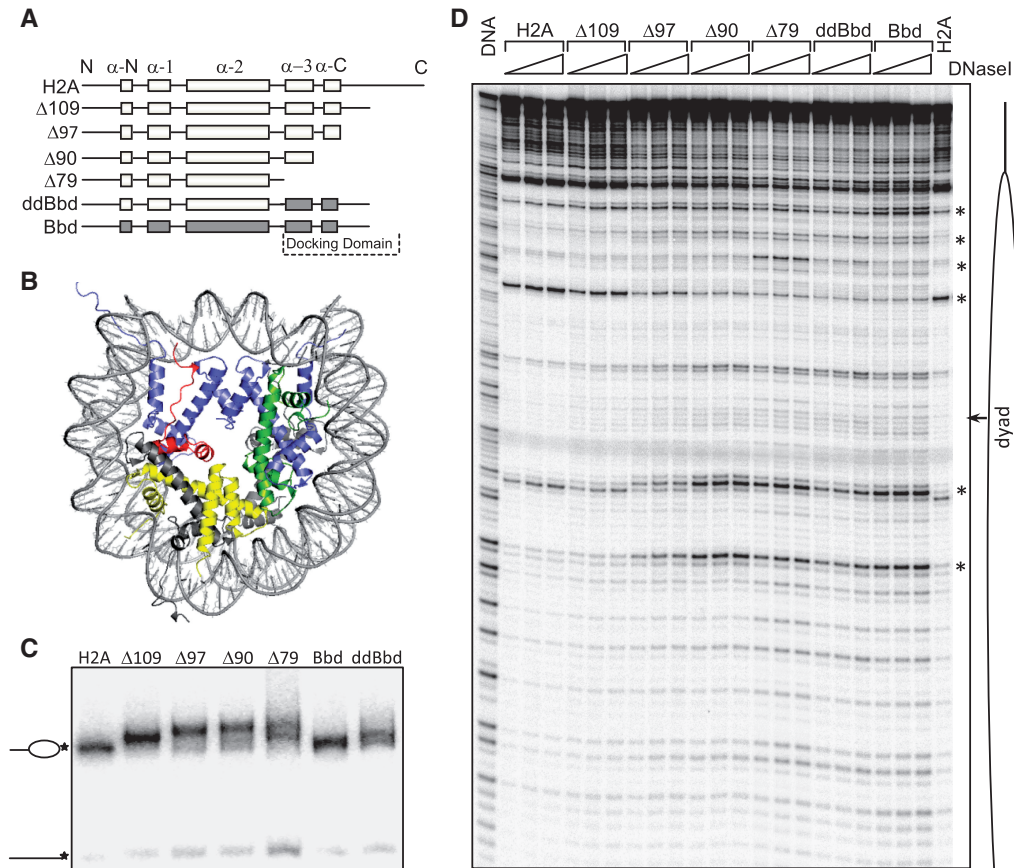
Figure 1. Biochemical characterization of conventional, variant and mutant nucleosomes. (**A**) Cartoon drawing of H2A mutants used in the study. In H2A.ddBbd chimeric protein the docking domain and the last C-terminal part was replaced with docking domain of H2A.Bbd. (**B**) Structure of the NCP, modified from (1), to show the H2A docking domain within the NCP. H2A, H2B, H3 and H4 are shown in grey, yellow, blue and green, respectively. The docking domain of H2A (amino acids 82–118) is colored in red. (**C**) EMSA of the end-positioned conventional (lane 1), variant (lane 6), chimeric (lane 7) and mutant (lanes 2–5) nucleosomes reconstituted on 205 bp ^{32}P-3′-labeled 601 DNA fragment. The 3′-^{32}P-labeled position is indicated by an asterisk. Positions of nucleosomes and free DNA are indicated at the left of the figure. (**D**) DNase I footprinting of the nucleosomes described in (C). Nucleosomes were digested with increasing amount of DNase I (0.2, 0.3 and 0.45 units) for 2.5 min at room temperature (lanes 2–23). Free DNA (lane DNA) was digested with 0.01 units of DNase I under the same conditions. Major structural perturbations are indicated by asterisk. Position of nucleosomal dyad is indicated.

purified. The recombinant proteins were analyzed by 18% SDS-PAGE (Supplementary Figure S1B). Next, we used these recombinant proteins for nucleosome reconstitution. For this, nucleosome reconstitutions were performed using a salt-dialysis method and by replacing conventional H2A with mutant proteins in the reconstitution mixtures containing all four core histones and a 205-bp 601 DNA fragment. This DNA fragment strongly positions nucleosomes at one end and is an ideal substrate for DNase I based footprinting assays. Under the reconstitution conditions, very little free DNA was observed (with the exception of Δ79 nucleosomes where the amount of free DNA was slightly higher), thus demonstrating efficient incorporation of mutant histones and reconstitution of *bona fide* nucleosomes in each case (Figure 1C). Note that the nucleosomes-containing deletion mutants of H2A exhibit a slower migration in the gel and this tendency increases with successive deletion in the COOH-terminal region. We attribute this to changes in conformation of linker DNA, which affects the migration in the gel (see below).

To test if the nucleosomes containing mutant and chimeric H2A exhibited, as suggested by their altered migration in native gel (Figure 1C), alterations in their structure, we have performed DNase I footprinting assays (Figure 1D). DNase I digestion of canonical nucleosomes gives a canonical 10-bp repeat, (19), indicative of the locations where the minor groove of nucleosomal DNA faces away from the histone surface and towards the solution. Incorporation of H2A Δ109 in the nucleosome showed no major structural perturbations. However, subtle changes were observed in the vicinity of nucleosomal dyad. Further deletions of COOH terminal residues, i.e. H2A Δ97, which lacks the C-terminal section of the docking domain, and H2A Δ90, which lacks all of the COOH-terminal region as well as the last α-helix of the docking domain, result in clear perturbation in the conformation of nucleosomal DNA. Similar perturbations are also seen when all of H2A COOH- terminal region as well the both α-helices of the docking domain were deleted in nucleosomes-containing H2A Δ79, or when the H2A-docking domain was replaced with docking domain

of H2A.Bbd (H2A.ddBbd nucleosomes). Interestingly, nucleosomes containing H2A.ddBbd yield a DNase I digestion profile nearly identical to H2A.Bbd nucleosomes.

In parallel, we performed •OH footprinting (Supplementary Figure S1C) on the same nucleosomes. All the nucleosomes show, as expected, a 10-bp repeat. The progressive deletion of the COOH-terminus of H2A affected, however, the quality of the •OH digestion pattern, i.e. the contrast in the pattern decreased with increasing the length of the COOH-deleted sequence, with the $\Delta79$ nucleosome being weaker compared to the parental H2A nucleosome pattern. Note that both H2A.Bbd and H2A.ddBbd nucleosomes exhibited •OH digestion profiles very similar to that of $\Delta79$ nucleosome. The DNase I and the •OH-footprinting data, taken together, demonstrate that the lack of the docking domain or the presence of the docking domain of H2A. Bbd led to prominent structural perturbations within the nucleosomes.

The docking domain of H2A stabilizes DNA wrapping throughout the nucleosome

To further study the role of the docking domain of H2A in the structure of the nucleosome, we used the 'one pot' assay to measure restriction enzyme accessibility all

along nucleosomal DNA in a single digestion reaction (39). Briefly, eight mutated 278-bp 601.2 DNA fragments [where each yields the same nucleosome positioning but has a unique *Hae* III restriction site, designated dyad-0 (d_0) to d-7 (d_7), where the number indicates the number of helical turns from the dyad, see schematics, Figure 2A] (39), were mixed in an equimolar ratio and used to reconstitute either conventional or chimeric H2A.ddBbd nucleosomes. The reconstitutions were then digested with 5 U/μl *Hae* III at different time points and the digested DNA was purified and separated on a sequencing gel (Figure 2B). After exposure of the dried gel, product bands from the experiment were quantified and expressed as percentage of cut fractions (Figure 2C).

The accessibility of d-7 (which is at the end of the core particle DNA) of the conventional H2A nucleosome differed from the other sites, since at the very initial points ∼90% of this site was cleaved. A typical dynamic accessibility at d-6 was also observed, where ∼8–10% of this site was cleaved and reaches ∼50% at the longest time of digestion (Figure 2B, lanes 1–6 and C). All the other *Hae* III sites were inaccessible to the restriction enzyme, in complete agreement with previous works (39,40). The picture is, however, completely different for the chimeric H2A.ddBbd nucleosomes (Figure 2B, lanes 8–13 and C).
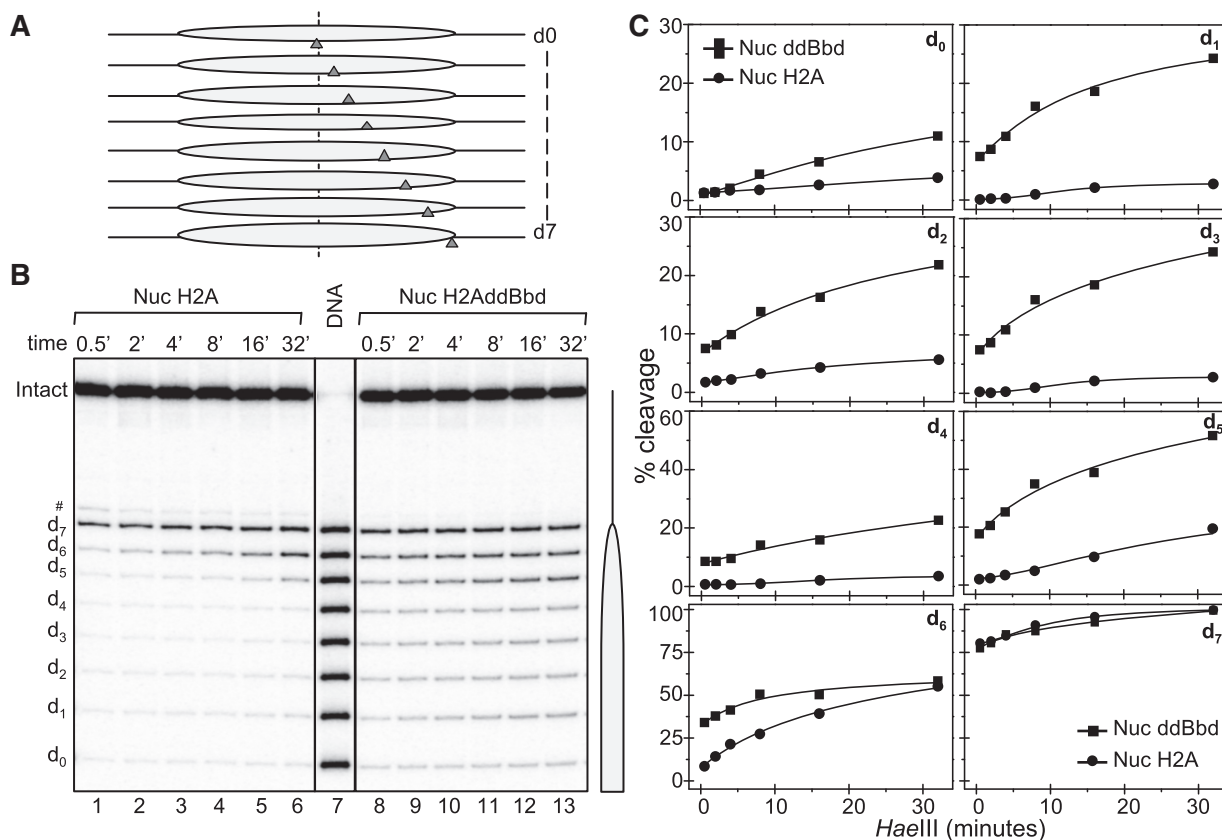

Figure 2. One pot restriction accessibility assay of conventional and chimeric H2A.ddBbd nucleosomes. Both types of nucleosomes were digested with 5 U/μl *Hae* III for the times indicated and after arresting the reaction, the digested DNA was purified and run on a 8% PAGE under denaturing conditions. (**A**) Schematics of the one pot assay. (**B**) The gel shows Hae III digestion profile of conventional (lanes 1–6) and chimeric H2A.ddBbd (lanes 8–13) nucleosomes. Lane 7 represents naked DNA digested 0.5 U/μl *Hae* III. On the right part a drawing of the nucleosome is shown. (**C**) *Hae* III digestion profile of conventional (circles) and chimeric H2A.ddBbd (squares) nucleosomes, quantified from the gel image presented in (B).

Indeed, all the *Hae* III sites within the nucleosomal core showed significant accessibility even at the shorter time points of digestion. This accessibility reaches up to ~20–25% for sites 1–4. Site 5 was also much more accessible compared to canonical H2A nucleosomes, where ~20% of this site was cleaved in initial time points and reached to ~50% in highest time point. We attributed this effect as reflecting structural perturbations in histone–DNA interactions throughout the chimeric H2A.ddBbd nucleosomes. H2A.Bbd-containing nucleosomes showed a similar overall increase in accessibility profile (Supplementary Figure S2). Taken together, this indicates that the structural changes observed in the H2A.Bbd nucleosomes can be attributed to its defective domain to a large extent.

The H2A-docking domain stabilizes the wrapping of one helical turn of DNA around the histone octamer at each edge of the nucleosome

The chimeric H2A.ddBbd nucleosomes showed altered DNase I and •OH cleavage patterns as well as marked increases in *Hae* III accessibility all along the nucleosomal DNA. All these features are reminiscent of nucleosomes containing H2A.Bbd (16,17,19). Since H2A.Bbd nucleosomes are complexed with only ~130 bp of DNA, which in turn affects the entry/exit angle of the linker DNA (19), we wondered whether the H2A.ddBbd nucleosomes exhibited similar characteristics. We approached this question by using Atomic Force Microscopy (AFM).

We used AFM to measure the length of DNA complexed (*Lc*) with the histone octamer in both conventional and H2A.ddBbd nucleosomes, centrally positioned on a 255-bp 601 DNA fragment (Figure 3A and B). Nucleosomes on this fragment exhibit two relatively long free DNA linkers, whose length can be precisely measured by AFM (21). This allows us to calculate both the length of DNA in complex with the histone octamer L_c ($L_c = L_{tot} - L_+ - L_-$, where $L_{tot} = 255$ bp, the length of the 601 fragment used for reconstitution, L_+ and L_- are the lengths of the DNA linkers, as measured from AFM images) and the variation relative to the DNA center position of the nucleosome $\Delta L = {}_{(}L_+ - L_-)/2$ (21). The data show that the H2A.ddBbd nucleosome is associated with only ~130-bp DNA, in contrast to the conventional nucleosome, determined to be associated with 146-bp DNA (Figure 3C). Note that the positions of both the conventional and the H2A.ddBbd nucleosomes were identical (Figure 3D). We conclude that the defective docking domain present in the H2A.ddBbd nucleosome affect the wrapping of ~10 bp of each end of the nucleosomal DNA but not the sequence-dependent positioning of the nucleosome on the DNA fragment.

The docking domain of histone H2A is required for proper histone H1 binding to the nucleosome

If the wrapping of the DNA is affected in H2A.ddBbd nucleosomes, which is especially pronounced at the ends, one should expect the entry/exit angle of nucleosomal DNA to be strongly altered and which might in turn affect the ability of linker histone to properly bind to nucleosomes. We next examined this feature using Elecrophoretic Mobility Shift Assay (EMSA), •OH footprinting and EC-M.

First, we employed EMSA to examine the binding of linker histone H1 to mononucleosomal substrates. Nucleosomes containing either conventional H2A or chimeric H2A.ddBbd histones were reconstituted on a ^{32}P-labeled 189-bp 601 DNA sequence, which yields centrally positioned nucleosomes with 21 bp of linker DNA on either side of the nucleosome. Next, we used the method of Nap1-facilitated deposition of H1 on these nucleosomes (41). An increasing amount of H1–Nap1 complex (in a molar ratio of 1:2) was then added to H2A, H2A.Bbd and H2A.ddBbd nucleosomes. The binding reaction products were resolved on a 2% agarose gel (Figure 4A). As seen, the binding of H1 to conventional nucleosomes resulted in a well-defined band with slower electrophoretic mobility (Figure 4A, left panel), in agreement with previous results (41). However, in the case of H2A.Bbd nucleosomes, the electrophoretic pattern was somewhat different. Indeed, the presence of H1 induces a very diffuse band with slower electrophoretic mobility as well as a smearing all along the length of the gel (Figure 4A, middle panel). The picture was very similar in the case of H2A.ddBbd nucleosomes (Figure 4A, right panel). Also, a higher level of aggregation was observed in case of H2A.Bbd and H2A.ddBbd nucleosomes, suggesting improper binding of H1 to these nucleosomes.

To further examine H1 binding to these nucleosomes, we next employed hydroxyl radical footprinting. *Bona fide* binding of H1 to nucleosomes results in two characteristic alterations in the hydroxyl radical cleavage profile: a clear protection at the nucleosomal dyad and appearance of a 10-bp repeat structure in the linker DNA (32). We reconstituted H2A, H2A.Bbd and H2A.ddBbd dinucleosomes on a 423-end labeled DNA. Linker histone H1 was deposited on these dinucleosomal substrates as described above (also see Material and methods section) and •OH footprinting was performed (Figure 4B). As expected, each one of the nucleosomes exhibits a 10-bp repeat in the region organized by the histone octamer and a random cleavage profile similar to naked DNA within the linker DNA region (Figure 4B lanes 1, 3 and 5; also see the lane scans in Supplementary Figure S3). The binding of linker histone H1 on the dinucleosomes-containing canonical H2A results in a clear footprint at the nucleosomal dyad as well as an appearance of 10-bp-repeat structure in the linker DNA (Figure 4B, lane 2 and Supplementary Figure S3). The picture was, however, completely different in the case of H2A.Bbd and H2A.ddBbd nucleosomes where neither of these characteristic features were obtained upon H1 deposition (Figure 4B, lanes 4 and 6 and Supplementary Figure S3). The •OH cleavage profile remains essentially similar as in the absence of H1, clearly indicating that the absence of a canonical-docking domain results in complete abrogation of proper H1 binding to the nucleosomes. These results were further confirmed by visualization of H2A and H2A.ddBbd trinucleosomes by EC-M (Figure 4C). Typically, proper binding of linker histone
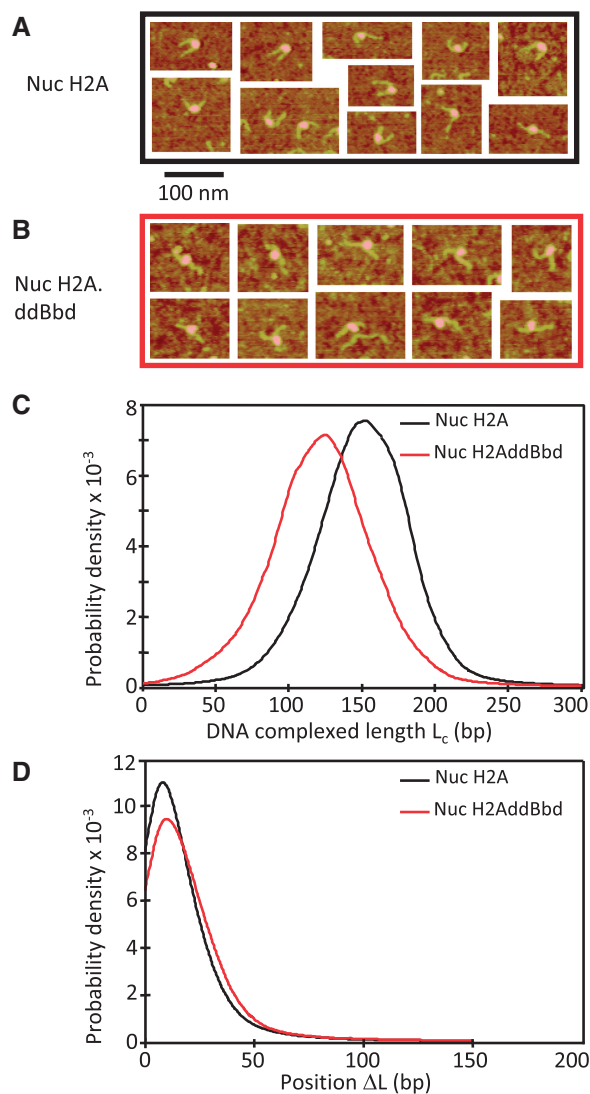
A

Nuc H2A

100 nm

B

Nuc H2A.
ddBbd

C

D

Figure 3. AFM imaging of conventional (H2A) and chimeric H2A.ddBbd nucleosomes. A 255-bp 601 DNA sequence was used to reconstitute centrally positioned conventional and H2AddBbd nucleosomes. The nucleosome samples were then visualized by AFM. Representative AFM images for the conventional (nuc H2A) and chimeric (nuc H2AddBbd) nucleosomes are shown in (**A**) and (**B**), respectively. (**C**) The complexed DNA length (L_c) distribution for conventional and H2AddBbd nucleosomes is presented. Note that Lc peaks at ~130 and ~150 bp for the H2A.ddBbd and conventional nucleosomes, respectively. (**D**) Nucleosome position (DL) distribution for conventional and H2AddBbd nucleosomes. The numbers of particles used for the calculation of the distributions were $N = 3247$ and 971 for conventional and H2A.ddBbd nucleosomes, respectively.

to nucleosomes or to nucleosomal arrays results in a specific spatial orientation of entry–exit DNA and the linker DNAs become juxtaposed to form a stem like structure (32,42). As expected, in the case of conventional H2A-containing trinucleosomes, the addition of H1 results in pulling together of incoming and outgoing linker DNAs towards the dyad axis (Figure 4C, upper panel). This leads to the formation of typical 'stem structure' (indicated by white arrows). Importantly, these H1-trinucleosome complexes were indistinguishable from

native H1-containing chromatin (42). The picture is, however, completely different in case of H2A.ddBbd containing trinucleosomes where no such stem structure was obtained in presence of H1 and the trinucleosomes retain their 'beads on string structure' with no change in entry–exit angle of DNA (Figure 4C, lower panel).

Taken together, these data clearly demonstrate that the docking domain of H2A is critical for the proper binding of H1 to nucleosomal substrates.

The docking domain of H2A is required for both nucleosome remodeling and mobilization by RSC

It is well documented that H2A.Bbd-containing nucleosomes are refractory to SWI/SNF and ACF mediated remodeling and mobilization (16,19) as well as heat induced mobilization (17). Moreover, the observation that truncations in the H2A COOH-terminal domain and swapping the H2A-docking domain with that of H2A.Bbd resulted in perturbations similar to H2A.Bbd-containing nucleosomes led us to test whether these structural changes affect the capacity of RSC to act on nucleosomes. We first concentrated on nucleosome remodeling. To this end, we incubated the reconstituted nucleosomes (Figure 1) for different times with RSC in the presence of ATP. After arresting the remodeling reaction, the samples were digested with DNase I and the DNA analyzed on 8% sequencing gels (Figure 5). The prolonged incubation with RSC resulted in alterations of the DNase I cleavage pattern of conventional nucleosomes as several new bands corresponding to free DNA were observed. These changes in the cleavage pattern indicate efficient ATP-dependent remodeling by RSC, resulting in perturbations of the histone–DNA contacts (43). Upon incubation with RSC, very similar changes in the DNase I cleavage pattern were observed for Δ109, Δ97 and Δ90 nucleosomes. However, in Δ90 nucleosomes, the remodeling efficiency is reduced compared to nucleosomes containing full length H2A. Similarly, for the Δ79, H2A.ddBbd and H2A.Bbd particles, the efficiency of remodeling is progressively weakened (see the regions marked by asterisks). These results indicate a requirement for the H2A C-terminal region and especially the docking domain for efficient RSC remodeling of nucleosomes. Note that some structural alterations within the non-RSC treated Δ79, H2A.ddBbd and H2A.Bbd particles, reminiscent of these of the remodeled H2A, Δ109, Δ97 and Δ90 particles, were also observed. The DNase I digestion pattern within these regions did not change after treatment with RSC (Figure 5, see the regions marked by φ in the RSC 0′ time control of these particles). This indicates the RSC activity on docking domain-deficient nucleosome results in a different conformation of remodeled species.

We next determined whether the H2A-docking domain is required for RSC-induced nucleosome mobilization. In this case, centrally positioned 601 nucleosomes were incubated with increasing amounts of RSC and the reaction products were resolved on 5% native PAGE (Figure 6A). Conventional H2A-containing nucleosomes are slid efficiently by RSC (Figure 6A and B). Indeed,
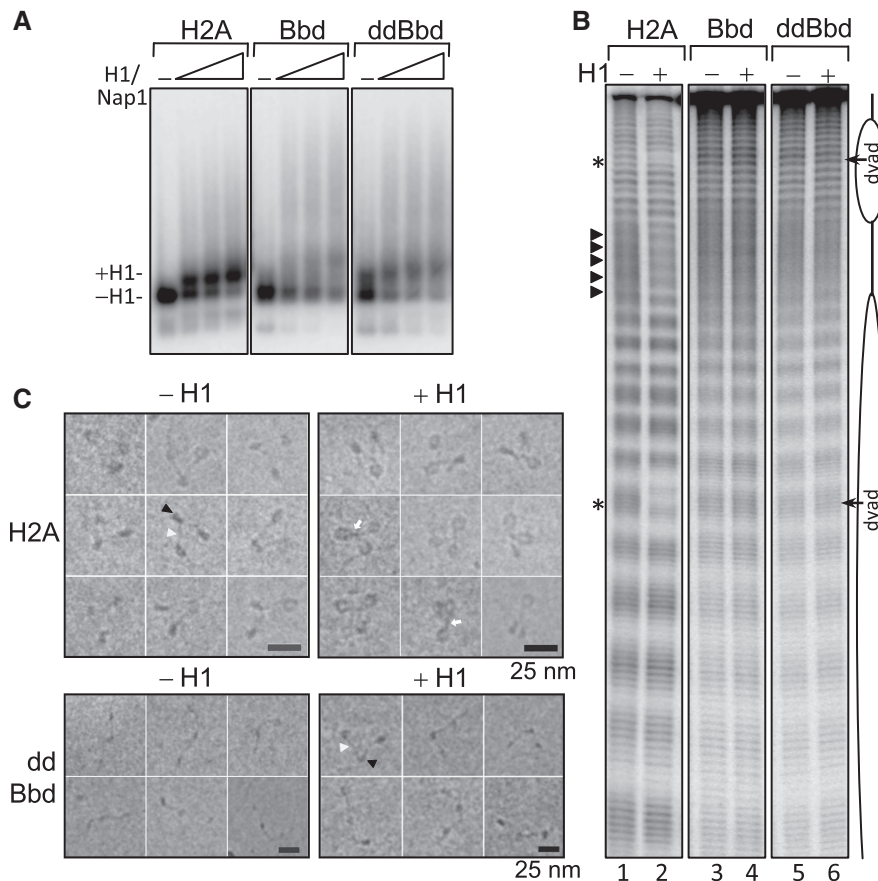
Figure 4. Examining linker histone H1 binding on mono and dinucleosomal substrates containing canonical, H2A.Bbd or H2A.ddBbd proteins. (**A**) EMSA to analyze the deposition of linker histone H1 on mononucleosomes. ^{32}P-body-labeled 189-bp 601 DNA sequence was used to reconstitute centrally positioned nucleosomes containing conventional H2A, H2A.Bbd or H2A.ddBbd chimeric protein. Increasing concentrations of H1/Nap1 complex (1:2 molar ratio) were added to the nucleosomes. Positions of nucleosomes with or without bound H1 are denoted by arrows on the left. (**B**) Hydroxyl radical footprinting to examine the binding of H1 on dinucleosomes. Lane 1, 3 and 5 show control dinucleosomes containing H2A, H2A.Bbd and H2A.ddBbd respectively in absence of H1. Lanes 2, 4 and 6; same dinucleosomes in presence of H1. Respective positions of nucleosomes and linker DNAs are denoted by cartoon drawing. •OH cleavage protection at the dyad and 10-bp repeat structure in the linker are shown by asterisks and triangles, respectively. (**C**) Representative EC-M images of reconstituted conventional and H2A.ddBbd trinucleosomes in absence (left panels) or in presence of linker histone H1 (right panels). A DNA-fragment containing three tandem repeats of 601 positioning sequence was used for reconstitution. The nucleosome and the linker DNA are indicated by black and white arrowheads, respectively. Note that the conventional nucleosomes exhibit, in agreement with the reported data, a typical equilateral triangle shape with two nucleosomes located at each end of the trinucleosomal DNA and a middle nucleosome. In contrast, the H2A.ddBbd trinucleosome particles, show a relaxed 'beads on a string' structure (lower row), evidencing for a perturbed 3D organization and changes in the entry/exit angle of the nucleosomal DNA ends.

2.4 U of RSC were sufficient to slide nucleosomes to saturation in 45 min. However, COOH-terminal truncations of H2A profoundly reduced the efficiency of RSC mediated nucleosome mobilization (Figure 6A and B). For example, upon incubation with 1.2 U of RSC, ~60% of canonical nucleosomes, and only ~30% and ~15% of Δ97 and Δ90 nucleosomes were slid, respectively (Figure 6B). Even with highest amount of RSC the reduction in sliding efficiency on these nucleosomes is clearly seen (Figure 6B). Note that RSC was completely unable to mobilize Δ79 and H2A.ddBbd nucleosomes (Figure 6A and B). We conclude that the docking domain of H2A is required for nucleosome mobilization by RSC.

DISCUSSION

Our data indicate that the H2A-docking domain is a key structural component of nucleosomes. We show that

deletion of this domain or replacement with the shortened and highly variant docking domain of H2A.Bbd results in significant alterations in nucleosome structure as detected by DNAse I and •OH footprinting, AFM measurements and cryo-EM analyses. Indeed, due to its key role in defining canonical nucleosome structure, the docking domain is required for proper binding of linker histone to the nucleosome and for efficient ATP-dependent re-modeling and nucleosome mobilization by the RSC complex. Moreover, our data suggest that a primary structural role of H2A.Bbd may be the inclusion of a 'defective' docking domain within specific nucleosomes *in vivo*.

X-ray crystal structures of nucleosomes suggests that the docking domain (82–119 AA) of H2A is involved in organizing the last turn of nucleosomal DNA through guiding the H3αN helix (1). In addition, the short α-C helix (amino acids 92–96) of the H2A-docking domain forms a short β sheet interaction with COOH-terminal
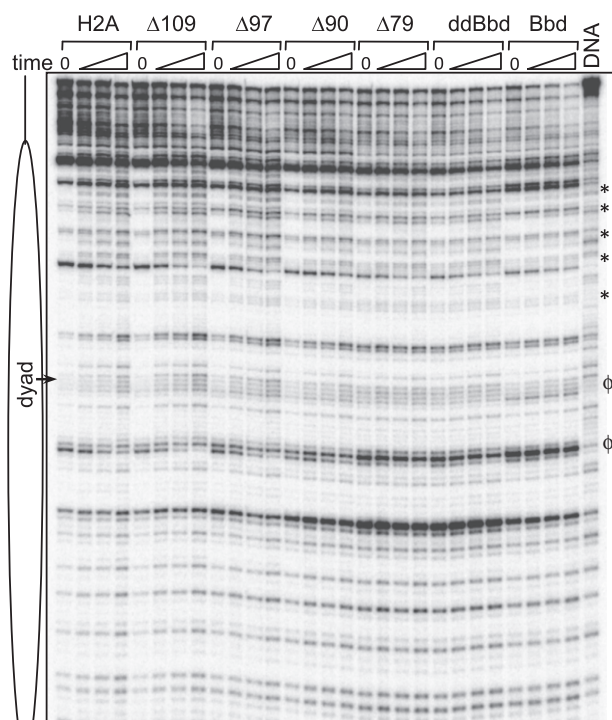
Figure 5. RSC-induced remodeling of conventional, truncated H2A mutants, H2A.ddBbd (ddBbd) and H2A.Bbd nucleosomes. The indicated end-positioned nucleosomes were reconstituted on a ^{32}P-3′-labeled 205-bp 601 DNA fragment and incubated for increasing times (from 0 to 62 min) at 29°C with 2.4 units of RSC. The reactions were arrested and, after digestion of the samples with DNase I, the cleaved DNA was extracted and run on an 8% PAGE under denaturing conditions. DNA, the DNase I digestion pattern of free DNA; the asterisks show the major changes in the DNase I digestion profile. Alterations specific RSC untreated Δ79, H2A.ddBbd and H2A.Bbd nucleosomes are marked by ϕ. Position of the dyad is indicated.

Figure 6. The docking domain of H2A is essential for the mobilization of the nucleosomes by RSC. (**A**) Centrally positioned conventional H2A (upper row, left panel), Δ109 (upper row, middle panel), Δ97 (upper row, right panel), Δ90 (lower row, left panel), Δ79 (lower row, middle panel) and H2A.ddBbd (lower row, right panel) reconstituted on a 255-bp 601 DNA were incubated with increasing amounts of RSC (as indicated) in presence of 1 mM ATP for 45 min at 29°C. Reactions were stopped by addition of 0.01 units of apyrase. Samples were resolved on 5% native PAGE. Gels were dried and visualized by exposure on a PhosphorImager. Positions of unmobilized and slid nucleosomes in the gel are shown by cartoon drawing. (**B**) Quantification of gel data for conventional H2A, Δ109, Δ97 and Δ90, Δ79 and H2A.ddBbd nucleosomes presented in A.

region of H4 (amino acids 95–102), suggesting this interaction contributes to (H2A–H2B)$_2$ dimer-(H3-H4)$_4$ tetramer stability within the nucleosome. Thus lack of a docking domain or the presence of a 'defective' docking domain is thus expected to strongly affect the structural organization of the nucleosome (1). Our data show that this is the case. Indeed, a progressive appearance of specific bands in DNase I profile concomitant with the progressive deletion of COOH-terminal region of H2A was observed. The chimeric H2A.ddBbd nucleosome, containing the 'defective' docking domain of H2A.Bbd, exhibited a DNase I digestion pattern very similar to the Δ79 H2A nucleosome, which completely lacks the docking domain of H2A. Importantly, the H2A.ddBbd particle is associated with only ∼130 bp of DNA, in contrast to the conventional particle, which organizes 147 bp of DNA. The AFM data show that within the H2A.ddBbd ∼10 bp of each end of the nucleosomal DNA are unwrapped. In agreement with this, the EC-M imaging demonstrated that the entry–exit angle of the H2A.ddBbd nucleosomal DNA is strongly altered and the H2A.ddBbd trinucleosomes have a 'relaxed' beads-on-a string structure in contrast to the equilateral triangle shape of the conventional trinucleosome (Figure 4 C).
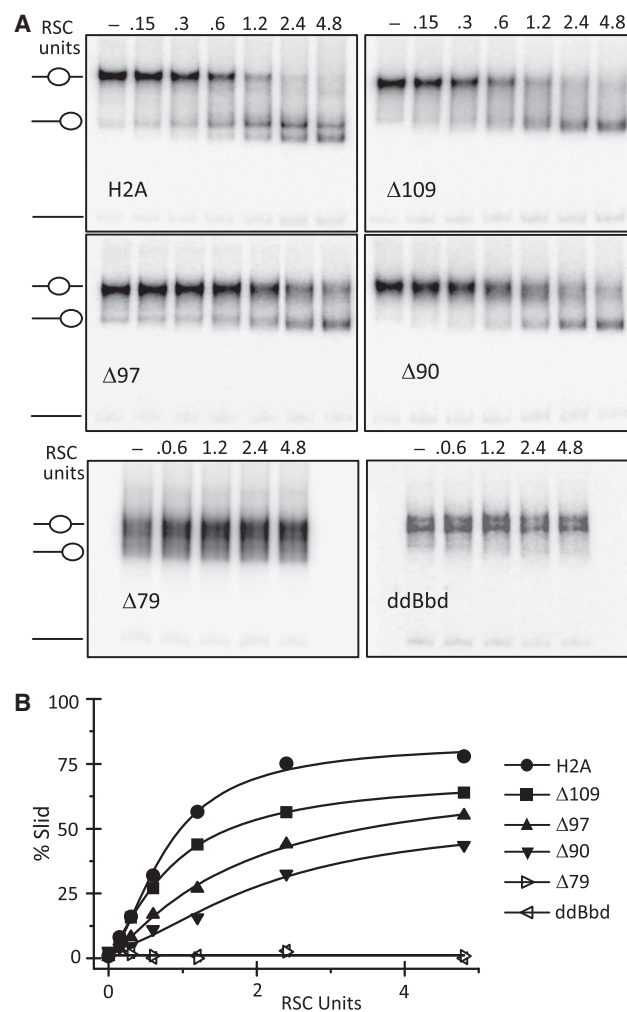
The structural perturbations brought about by deletion of the docking domain or the 'defective' H2A.Bbd-docking domains are associated with the inability of RSC to both remodel and mobilize the nucleosomes. Interestingly, similar effects on RSC induced sliding were observed when mutations were incorporated in the histone H3 αN region (44). Note that the (H3-H4)$_2$ tetramer-DNA particle is also not mobilized by the SWI/SNF chromatin remodeling complex (M. S. Shukla, D. Angelov and S. Dimitrov, unpublished data), providing further evidence that the presence of (H2A–H2B) dimers with a canonical docking domain interacting in a native fashion with the (H3-H4)$_2$ tetramer are required for the mobilization process. However, it has

been shown that SWI/SNF, an ATP-dependent remodeler of the same family, was able to remodel H3-H4 tetramer arrays resulting in increased accessibility to restriction enzyme although with considerably less efficiency (45). These results are consistent with our remodeling data where weak remodeling by RSC was detected in the DNAse I assay for Δ79, H2A.ddBbd and H2A.Bbd, while RSC was unable to mobilize nucleosomes containing these proteins.

A current model of nucleosome mobilization by ATP-dependent chromatin remodelers involves DNA-bulge propagation within the nucleosome perhaps initiated via a 'loop recapture' mechanism (46–48). Considering this view, the weaker interactions between DNA at the periphery of the nucleosome core due to a presence of a truncated or defective docking domain may reduce the probability of loop recapture and thus hamper the ability of the ATP-dependent remodelers to mobilize the nucleosomes, consistent with our observations (Figure 6). Alternatively, the distorted conformation due to the altered docking domain may negatively impact recognition and binding of the nucleosome substrate by the RSC-remodeling complex. We note that although we have used RSC as a model chromatin remodeler in this study, one should expect a similar structural dependence by remodelers belonging to other families. Indeed, H2A.Bbd nucleosomes are also refractory to ACF induced mobilization (16).

We also found that the docking domain of H2A appears to be critically important for proper binding of linker histone H1. Linker histones preferentially bind to four-way junction (4WJ) DNA compared to linear DNA. This preferential binding of linker histones to 4WJ DNA was attributed to the particular angle formed between the two DNA arms (49). Bearing this in mind, one could expect that the specific 3D organization of the incoming–outgoing linkers would be critical for binding of H1. In H2A.ddBbd containing nucleosomes, where the H2A-docking domain is 'defective', one of the major structural effects was on the entry–exit angle of linker DNAs. Consistent with this, a complete abrogation of H1 proper binding was observed (Figure 4 and Supplementary Figure S3) emphasizing the role of H2A-docking domain in H1-mediated condensation of chromatin.

Interestingly, the incorporation of the histone variant H2B.FWT, which shows a highly divergent (45% identity) primary structure compared to this of the conventional H2B, did not interfere with chromatin remodeler-mediated nucleosome mobilization (50). This reinforces the notion for the unique role of H2A and its docking domain in the mobilization of the nucleosomes. This specific property of H2A allows the creation of nucleosomes with specific structural and functional properties upon the incorporation of variants such as H2A.Bbd and perhaps H2AL2 (16,17,21). Nucleosomes containing either protein cannot be mobilized and the reported data indicate that transcription and repair are more facile on H2A.Bbd nucleosomal templates (12,16,51). In addition, H2A.Bbd nucleosomal arrays exhibit 'beads on a string' structure, in contrast to the conventional H2A arrays, which show specific local organization (11). Moreover,

H2A.Bbd arrays were unable to fold properly upon raising the ionic strength of the solution (12). H2A.Bbd seems to be associated with transcriptionally active chromatin (31) and, as well as H2AL2 (21) in the processes taking place during spermatogenesis (52). Therefore, this histone H2A variant structure–function relationship and, in particular the peculiar structural role of the H2A-docking domain, appears to be exploited by the cell to regulate such vital processes as transcription and spermatogenesis.

SUPPLEMENTARY DATA

Supplementary Data are available at NAR Online.

FUNDING

Conflict of interest statement. None declared.

REFERENCES

1. Luger,K., Mäder,A.W., Richmond,R.K., Sargent,D.F. and Richmond,T.J. (1997) Crystal structure of the nucleosome core particle at 2.8 A resolution. *Nature*, **389**, 251–260.
2. van Holde,K. (1988) Chromatin. Springer-Verlag KG, Berlin, Germany.
3. Sivolob,A. and Prunell,A. (2003) Linker histone-dependent organization and dynamics of nucleosome entry/exit DNAs. *J. Mol. Biol.*, **331**, 1025–1040.
4. Fan,Y., Nikitina,T., Zhao,J., Fleury,T.J., Bhattacharyya,R., Bouhassira,E.E., Stein,A., Woodcock,C.L. and Skoultchi,A.I. (2005) Histone H1 depletion in mammals alters global chromatin structure but causes specific changes in gene regulation. *Cell*, **123**, 1199–1212.
5. Arents,G. and Moudrianakis,E.N. (1995) The histone fold: a ubiquitous architectural motif utilized in DNA compaction and protein dimerization. *Proc. Natl Acad. Sci. USA*, **92**, 11170–11174.
6. Smirnov,I.V., Dimitrov,S.I. and Makarov,V.L. (1988) NaCl-induced chromatin condensation. Application of static light scattering at 90 degrees and stopped flow technique. *J. Biomol. Struct. Dyn.*, **5**, 1127–1134.
7. Makarov,V.L., Dimitrov,S.I., Tsaneva,I.R. and Pashev,I.G. (1984) The role of histone H1 and non-structured domains of core histones in maintaining the orientation of nucleosomes within the chromatin fiber. *Biochem. Biophys. Res. Commun.*, **122**, 1021–1027.
8. de la Barre,A.E., Angelov,D., Molla,A. and Dimitrov,S. (2001) The N-terminus of histone H2B, but not that of histone H3 or

its phosphorylation, is essential for chromosome condensation. *EMBO J.*, **20**, 6383–6393.

9. Scrittori,L., Hans,F., Angelov,D., Charra,M., Prigent,C. and Dimitrov,S. (2001) pEg2 aurora-A kinase, histone H3 phosphorylation, and chromosome assembly in Xenopus egg extract. *J. Biol. Chem.*, **276**, 30002–30010.

10. Li,B., Carey,M. and Workman,J.L. (2007) The role of chromatin during transcription. *Cell*, **128**, 707–719.

11. Montel,F., Menoni,H., Castelnovo,M., Bednar,J., Dimitrov,S., Angelov,D. and Faivre-Moskalenko,C. (2009) The dynamics of individual nucleosomes controls the chromatin condensation pathway: direct atomic force microscopy visualization of variant chromatin. *Biophys. J.*, **97**, 544–553.

12. Zhou,J., Fan,J.Y., Rangasamy,D. and Tremethick,D.J. (2007) The nucleosome surface regulates chromatin compaction and couples it with transcriptional repression. *Nat. Struct. Mol. Biol.*, **14**, 1070–1076.

13. Becker,P.B. (2002) Nucleosome sliding: facts and fiction. *EMBO J.*, **21**, 4749–4753.

14. Boulard,M., Bouvet,P., Kundu,T.K. and Dimitrov,S. (2007) Histone variant nucleosomes: structure, function and implication in disease. *Subcell. Biochem.*, **41**, 71–89.

15. Strahl,B.D. and Allis,C.D. (2000) The language of covalent histone modifications. *Nature*, **403**, 41–45.

16. Angelov,D., Verdel,A., An,W., Bondarenko,V., Hans,F., Doyen,C.M., Studitsky,V.M., Hamiche,A., Roeder,R.G., Bouvet,P. *et al.* (2004) SWI/SNF remodeling and p300-dependent transcription of histone variant H2ABbd nucleosomal arrays. *EMBO J.*, **23**, 3815–3824.

17. Bao,Y., Konesky,K., Park,Y.J., Rosu,S., Dyer,P.N., Rangasamy,D., Tremethick,D.J., Laybourn,P.J. and Luger,K. (2004) Nucleosomes containing the histone variant H2A.Bbd organize only 118 base pairs of DNA. *EMBO J.*, **23**, 3314–3324.

18. Fan,J.Y., Rangasamy,D., Luger,K. and Tremethick,D.J. (2004) H2A.Z alters the nucleosome surface to promote HP1alpha-mediated chromatin fiber folding. *Mol. Cell*, **16**, 655–661.

19. Doyen,C.M., Montel,F., Gautier,T., Menoni,H., Claudet,C., Delacour-Larose,M., Angelov,D., Hamiche,A., Bednar,J., Faivre-Moskalenko,C. *et al.* (2006) Dissection of the unusual structural and functional properties of the variant H2A.Bbd nucleosome. *EMBO J.*, **25**, 4234–4244.

20. Doyen,C.M., An,W., Angelov,D., Bondarenko,V., Mietton,F., Studitsky,V.M., Hamiche,A., Roeder,R.G., Bouvet,P. and Dimitrov,S. (2006) Mechanism of polymerase II transcription repression by the histone variant macroH2A. *Mol. Cell. Biol.*, **26**, 1156–1164.

21. Syed,S.H., Boulard,M., Shukla,M.S., Gautier,T., Travers,A., Bednar,J., Faivre-Moskalenko,C., Dimitrov,S. and Angelov,D. (2009) The incorporation of the novel histone variant H2AL2 confers unusual structural and functional properties of the nucleosome. *Nucleic Acids Res.*, **37**, 4684–4695.

22. Jin,C. and Felsenfeld,G. (2007) Nucleosome stability mediated by histone variants H3.3 and H2A.Z. *Genes Dev.*, **21**, 1519–1529.

23. Abbott,D.W., Ivanova,V.S., Wang,X., Bonner,W.M. and Ausio,J. (2001) Characterization of the stability and folding of H2A.Z chromatin particles. Implications for transcriptional activation. *J. Biol. Chem.*, **276**, 41945–41949.

24. Gautier,T., Abbott,D.W., Molla,A., Verdel,A., Ausio,J. and Dimitrov,S. (2004) Histone variant H2ABbd confers lower stability to the nucleosome. *EMBO Rep.*, **5**, 715–720.

25. Suto,R.K., Clarkson,M.J., Tremethick,D.J. and Luger,K. (2000) Crystal structure of a nucleosome core particle containing the variant histone H2A.Z. *Nat. Struct. Biol.*, **7**, 1121–1124.

26. Jin,C., Zang,C., Wei,G., Cui,K., Peng,W., Zhao,K. and Felsenfeld,G. (2009) H3.3/H2A.Z double variant-containing nucleosomes mark 'nucleosome-free regions' of active promoters and other regulatory regions. *Nat. Genet.*, **41**, 941–945.

27. Redon,C., Pilch,D., Rogakou,E., Sedelnikova,O., Newrock,K. and Bonner,W. (2002) Histone H2A variants H2AX and H2AZ. *Curr. Opin. Genet. Dev.*, **12**, 162–169.

28. Ausio,J. and Abbott,D.W. (2002) The many tales of a tail: carboxyl-terminal tail heterogeneity specializes histone H2A

29. Ausio,J. (2006) Histone variants–the structure behind the function. *Brief. Funct. Genom. Proteom.*, **5**, 228–243.

30. Eickbush,T.H., Godfrey,J.E., Elia,M.C. and Moudrianakis,E.N. (1988) H2a-specific proteolysis as a unique probe in the analysis of the histone octamer. *J. Biol. Chem.*, **263**, 18972–18978.

31. Chadwick,B.P. and Willard,H.F. (2001) A novel chromatin protein, distantly related to histone H2A, is largely excluded from the inactive X chromosome. *J. Cell Biol.*, **152**, 375–384.

32. Syed,S.H., Goutte-Gattat,D., Becker,N., Meyer,S., Shukla,M.S., Hayes,J.J., Everaers,R., Angelov,D., Bednar,J. and Dimitrov,S. (2010) Single-base resolution mapping of H1-nucleosome interactions and 3D organization of the nucleosome. *Proc. Natl Acad. Sci. USA*, **107**, 9620–9625.

33. Luger,K., Rechsteiner,T.J. and Richmond,T.J. (1999) Expression and purification of recombinant histones and nucleosome reconstitution. *Methods Mol. Biol.*, **119**, 1–16.

34. Cairns,B.R., Lorch,Y., Li,Y., Zhang,M., Lacomis,L., Erdjument-Bromage,H., Tempst,P., Du,J., Laurent,B. and Kornberg,R.D. (1996) RSC, an essential, abundant chromatin-remodeling complex. *Cell*, **87**, 1249–1260.

35. Mutskov,V., Gerber,D., Angelov,D., Ausio,J., Workman,J. and Dimitrov,S. (1998) Persistent interactions of core histone tails with nucleosomal DNA following acetylation and transcription factor binding. *Mol. Cell. Biol.*, **18**, 6293–6304.

36. Hayes,J.J. and Lee,K.M. (1997) In vitro reconstitution and analysis of mononucleosomes containing defined DNAs and proteins. *Methods*, **12**, 2–9.

37. Montel,F., Fontaine,E., St-Jean,P., Castelnovo,M. and Faivre-Moskalenko,C. (2007) Atomic force microscopy imaging of SWI/SNF action: mapping the nucleosome remodeling and sliding. *Biophys. J.*, **93**, 566–578.

38. Angelov,D., Bondarenko,V.A., Almagro,S., Menoni,H., Mongelard,F., Hans,F., Mietton,F., Studitsky,V.M., Hamiche,A., Dimitrov,S. *et al.* (2006) Nucleolin is a histone chaperone with FACT-like activity and assists remodeling of nucleosomes. *EMBO J.*, **25**, 1669–1679.

39. Wu,C. and Travers,A. (2004) A 'one-pot' assay for the accessibility of DNA in a nucleosome core particle. *Nucleic Acids Res.*, **32**, e122.

40. Shukla,M.S., Syed,S.H., Montel,F., Faivre-Moskalenko,C., Bednar,J., Travers,A., Angelov,D. and Dimitrov,S. (2010) Remosomes: RSC generated non-mobilized particles with approximately 180 bp DNA loosely associated with the histone octamer. *Proc. Natl Acad. Sci. USA*, **107**, 1936–1941.

41. Shintomi,K., Iwabuchi,M., Saeki,H., Ura,K., Kishimoto,T. and Ohsumi,K. (2005) Nucleosome assembly protein-1 is a linker histone chaperone in Xenopus eggs. *Proc. Natl Acad. Sci. USA*, **102**, 8210–8215.

42. Bednar,J., Horowitz,R.A., Grigoryev,S.A., Carruthers,L.M., Hansen,J.C., Koster,A.J. and Woodcock,C.L. (1998) Nucleosomes, linker DNA, and linker histone form a unique structural motif that directs the higher-order folding and compaction of chromatin. *Proc. Natl Acad. Sci. USA*, **95**, 14173–14178.

43. Angelov,D., Molla,A., Perche,P.-Y., Hans,F., Cote,J., Khochbin,S., Bouvet,P. and Dimitrov,S. (2003) The histone variant macroh2a interferes with transcription factor binding and SWI/SNF nucleosome remodeling. *Mol. Cell*, **11**, 1033–1041.

44. Somers,J. and Owen-Hughes,T. (2009) Mutations to the histone H3 alpha N region selectively alter the outcome of ATP-dependent nucleosome-remodelling reactions. *Nucleic Acids Res.*, **37**, 2504–2513.

45. Boyer,L.A., Shao,X., Ebright,R.H. and Peterson,C.L. (2000) Roles of the histone H2A-H2B dimers and the (H3-H4)(2) tetramer in nucleosome remodeling by the SWI-SNF complex. *J. Biol. Chem.*, **275**, 11545–11552.

46. Kassabov,S.R., Zhang,B., Persinger,J. and Bartholomew,B. (2003) SWI/SNF unwraps, slides, and rewraps the nucleosome. *Mol. Cell*, **11**, 391–403.

47. Zhang,Y., Smith,C.L., Saha,A., Grill,S.W., Mihardja,S., Smith,S.B., Cairns,B.R., Peterson,C.L. and Bustamante,C. (2006)

DNA translocation and loop formation mechanism of chromatin remodeling by SWI/SNF and RSC. *Mol. Cell*, **24**, 559–568.

48. Strohner,R., Wachsmuth,M., Dachauer,K., Mazurkiewicz,J., Hochstatter,J., Rippe,K. and Langst,G. (2005) A 'loop recapture' mechanism for ACF-dependent nucleosome remodeling. *Nat. Struct. Mol. Biol.*, **12**, 683–690.

49. Varga-Weisz,P., Zlatanova,J., Leuba,S.H., Schroth,G.P. and van Holde,K. (1994) Binding of histones H1 and H5 and their globular domains to four-way junction DNA. *Proc. Natl Acad. Sci. USA*, **91**, 3525–3529.

50. Boulard,M., Gautier,T., Mbele,G.O., Gerson,V., Hamiche,A., Angelov,D., Bouvet,P. and Dimitrov,S. (2006) The NH2 tail of

the novel histone variant H2BFWT exhibits properties distinct from conventional H2B with respect to the assembly of mitotic chromosomes. *Mol. Cell. Biol.*, **26**, 1518–1526.

51. Menoni,H., Gasparutto,D., Hamiche,A., Cadet,J., Dimitrov,S., Bouvet,P. and Angelov,D. (2007) ATP-dependent chromatin remodeling is required for base excision repair in conventional but not in variant H2A.Bbd nucleosomes. *Mol. Cell. Biol.*, **27**, 5949–5956.

52. Ishibashi,T., Li,A., Eirin-Lopez,J.M., Zhao,M., Missiaen,K., Abbott,D.W., Meistrich,M., Hendzel,M.J. and Ausio,J. (2009) H2A.Bbd: an X-chromosome-encoded histone involved in mammalian spermiogenesis. *Nucleic Acids Res.*, **38**, 1780–1789.